Journal of Catalysis 276 (2010) 38–48

Contents lists available at ScienceDirect

Journal of Catalysis

journal homepage: www.elsevier.com/locate/jcat

TAP studies of CO oxidation over $CuMnO_X$ and $Au/CuMnO_X$ catalysts

Kevin Morgan [a], Kieran J. Cole [b], Alexandre Goguet [a], Christopher Hardacre [a,*], Graham J. Hutchings [b], Noleen Maguire [a], Sergiy O. Shekhtman [a], Stuart H. Taylor [b]

[a] *CenTACat, School of Chemistry and Chemical Engineering, Queen's University Belfast, Belfast BT 9 5AG, Northern Ireland, UK*
[b] *Cardiff Catalysis Institute, School of Chemistry, Cardiff University, Cardiff CF10 3TB, UK*

ARTICLE INFO

Article history:
Received 16 April 2010
Revised 28 July 2010
Accepted 24 August 2010

Keywords:
Temporal analysis of products
Hopcalite
Mechanism
Low temperature
Carbon monoxide
Oxidation

ABSTRACT

The mechanism of CO oxidation reactions over undoped and gold-doped $CuMnO_X$ (Hopcalite) catalysts has been examined using a temporal analysis of products (TAP) reactor. Gold doping has been found to increase the activity of the mixed oxide catalyst significantly; however, using consecutive pulsing TAP experiments, the presence of gold was not found to affect the contribution of the Langmuir–Hinshelwood mechanism. Conversely, gold doping was found to promote the Mars van Krevelen mechanism. Using CO and O_2 multi-pulse TAP experiments, the gold was found to modify the catalyst surface such that it stores much more oxygen that is active for the CO oxidation. The CO multi-pulse experiments indicated that two distinct types of active oxygen species were found to be involved in the CO oxidation. One type was observed in a similar amount on both doped and undoped catalysts and was associated with mixed oxide, while the second type was only found on the gold-doped catalyst and was therefore clearly associated with the presence of gold on the catalyst surface. The latter was found to be much less active than the oxygen inherent to the oxide but was at a concentration of approximately 10 times larger leading to the enhanced activity observed on gold doping.

1. Introduction

The catalytic oxidation of carbon monoxide at low temperature is an important reaction in applications including cold start exhaust emission control for automobiles, respirators, preferential oxidation of CO in the presence, for example, of hydrogen for pure hydrogen production [1]. Hopcalite, a mixed oxide of copper and manganese, has been effectively employed as a catalyst for the removal of CO for more than 80 years [2,3]. It has since been shown that when metal oxide catalysts are doped with precious metals, in particular gold, the activity of the catalyst can be improved [4].

Rogers et al. [3] investigated the low-temperature catalytic oxidation of CO and discovered that mixed oxides of MnO_2 with AgO or CuO were more active than any of the individual oxides. The first results indicated that the catalyst oxidised the CO before the catalyst was itself re-oxidised by oxygen from the air [2,3]. It was suggested that the mixed oxides were more active than the individual oxides because they could be more easily re-oxidised by molecular oxygen [3].

Recent results have shown that Au-doped Hopcalite catalysts displayed greater activities compared to the undoped samples [1].

There are two widely accepted possible reaction mechanisms for catalytic CO oxidation.

The Langmuir–Hinshelwood (LH) mechanism includes the following set of steps:

1. Competitive adsorption of reactant molecules from the gas phase onto the same surface.
2. Dissociation of the molecules on the surface.
3. Reaction between the adsorbed molecules/atoms.
4. Desorption of the reaction product(s) to the gas phase.

The alternative is the Mars van Krevelen (MvK) mechanism. The steps associated with this mechanism are as follows:

1. The metal/support is oxidised in a separate independent step.
2. CO molecules adsorbed on the oxide from the gas phase.
3. Absorbed CO reacts with surface oxygen atoms from the oxide.
4. Produced CO_2 desorbs from the surface.
5. The resulting oxygen vacancies are refilled rapidly and irreversibly by oxygen from the gas phase in separate step (1).

In the present work, a temporal analysis of products (TAP) reactor [5] was used to investigate how doping the mixed oxide with gold facilitates the CO oxidation reaction. The mechanism of CO oxidation over undoped and Au-doped Hopcalite $CuMnO_X$ catalysts was studied. In particular, the investigation focused on elucidating a possible role of Au doping in providing additional active sites or

---

* Corresponding author. Fax: +44 2890 974687.
E-mail address: c.hardacre@qub.ac.uk (C. Hardacre).

0021-9517/$ - see front matter © 2010 Elsevier Inc. All rights reserved.
doi:10.1016/j.jcat.2010.08.013

surface oxygen and examining the possible modification of the reaction mechanism.

2. Experimental

Following extensive previous work on this type of catalyst [1,6–8], which included activity tests and characterisation, two samples of the low-temperature CO oxidation catalysts were selected. The catalysts investigated in the current work were undoped $CuMnO_X$ and 0.5 wt.% Au-doped $CuMnO_X$. The $CuMnO_X$ catalyst was prepared by a co-precipitation method described in detail elsewhere [6]. The two starting solutions [0.25 M $Cu(NO_3)_2$ and $Mn(NO_3)_2$] were mixed to give an Mn/Cu atomic ratio of 2/1 and were precipitated at 80 °C with Na_2CO_3, filtered, washed and dried to produce the catalyst precursor. The precursor was calcined at 415 °C for 2 h to form the catalyst. The 0.5 wt.% Au was added onto the $CuMnO_X$ by deposition precipitation. The $CuMnO_X$ catalyst was suspended in distilled water at room temperature, and an appropriate amount of $HAuCl_4$ solution was added. The pH was raised to 9 by adding aqueous NaOH and the solution stirred vigorously for 1 h. The filtrate was recovered, washed thoroughly, dried at 120 °C for 16 h and then calcined at 400 °C for 3 h.

The catalytic activity was determined in a continuous flow fixed-bed quartz microreactor, operated at atmospheric pressure to ensure the catalyst samples had the appropriate activity for the pulse-flow reactor studies. The feed consisted of $CO:O_2:He$ with a molar ratio of 1:89:10. The combined flow rate was maintained at 22.5 ml/min over the catalyst (100 mg) at 25 °C. The two catalysts were tested for a minimum of 1000 min, and analysis of the reaction product was carried out online using gas chromatography. Conversion was calculated on the basis of CO_2 concentration in the effluent, and carbon balances were 100 ± 2%.

TAP pulse-response experiments were performed in the QUB TAP-1 reactor (Autoclave Engineers) using a stainless steel microreactor (41 mm long, 5.5 mm i.d.). Further details about the QUB TAP-1 reactor system are provided elsewhere [9,10]. In all experiments, the thin-zone TAP reactor (TZTR) concept [11] was used in order to maintain the catalyst composition approximately uniform during the whole course of TAP studies [12].

The microreactor was packed with a thin layer of catalyst (10 mg, 125–150 μm) sandwiched between two layers of inert silicon carbide (500 μm). The temperature of the reactor was measured by a thermocouple positioned in the centre of the microreactor. The reactant and product gases were recorded at the reactor outlet by a Hiden HAL V quadrupole mass spectrometer. The responses were analysed and modelled using moment-based analysis [13]. The TAP experiments were conducted at 100 °C in all cases in order for the pulse widths to be sufficiently narrow to be analysable. It should be noted that the Au-doped catalyst showed significantly higher steady-state activity over the temperature range 25–100 °C compared with the undoped catalyst. Therefore, despite the limitation that the TAP experiments had to be performed above ambient temperature, the mechanistic information provided at 100 °C is thought to be relevant to the low-temperature CO oxidation reaction over these catalysts.

For both catalysts, two main types of pulse-response TAP experiments were performed:

(1) A consecutive pulsing TAP experiment which has proven to be very effective in distinguishing reaction mechanisms (e.g. see [9] for details).
(2) A multi-pulse TAP experiment which enables the quantification of the number and the intrinsic activities of surface active species (e.g. see [10] for details).

The conditions for the consecutive pulse experiments are given below:

i. Oxidation of the catalyst by continuous flow of regular $^{16}O_2$ at 300 °C for 1 h.
ii. Evacuation of the reactor to 10^{-7} Torr.
iii. Pulsing of a 50/50 mix of $^{18}O_2/Ar$ followed by a 50/50 $^{13}CO/Ar$ mix after a specified time delay at a temperature of 100 °C.
iv. Time delays studied were 0 s, 0.5 s, 2 s and 4 s.

The experimental conditions and procedure of the multi-pulse studies are outlined below:

i. Oxidation of the catalyst by continuous flow of regular $^{16}O_2$ at 300 °C for 1 h.
ii. Evacuation of the reactor to 10^{-7} Torr.
iii. Pulsing of a 50/50 mix of $^{13}CO/Ar$ at 100 °C over the catalyst until no more CO consumption is observed (1st CO multi-pulse series).
iv. Pulsing of a 50/50 mix of O_2/Ar at 100 °C over the catalyst until no more O_2 consumption is observed (O_2 multi-pulse series).
v. Pulsing of a 50/50 mix of $^{13}CO/Ar$ at 100 °C over the catalyst again until no more CO consumption is observed (2nd CO multi-pulse series).

It should be noted that following the oxidation of the catalyst at 300 °C, but prior to the CO multi-pulse experiment, an oxygen multi-pulse experiment was conducted. No oxygen was consumed for either of the catalysts during this experiment, and thus no significant reduction of the surface upon exposure to vacuum was observed.

3. Results and discussion

The steady-state activity of the $CuMnO_X$ and the $Au/CuMnO_X$ catalysts along with their surface areas are shown in Table 1. Both catalysts demonstrated the characteristic deactivation of $CuMnO_X$ catalysts with time-on-stream [6], but reached steady-state CO conversion after *ca.* 100 min time-on-stream. The gold-doped catalyst was significantly more active than the undoped system reaching 55% conversion compared with 25% after 2 h time-on-stream. This difference in activity is not associated with a large change in BET surface area, for example, in fact the higher-activity sample has the smaller surface area.

Table 1
Ambient temperature steady-state CO oxidation activity and surface areas of $CuMnO_X$ and $Au/CuMnO_X$ catalysts.

Catalyst	BET surface area/m2 g^{-1}	CO conversion/%[a]
$CuMnO_X$	130	25
$Au/CuMnO_X$	105	55

[a] Steady-state activity after 2 h time-on-stream.

4. Consecutive pulse experiments

The purpose of the consecutive pulsing TAP experiments was to distinguish the contribution of the Langmuir–Hinshelwood (LH) and the Mars van Krevelen (MvK) mechanisms to the CO oxidation reaction over both catalysts (see [9] for the details). Using consecutive pulsing TAP experiments enables the surface oxygen supplied by the oxidative pre-treatment prior to the pulsing and oxygen adsorbed from the gas phase during the pulse experiment to be distinguished using isotopic labelling. During the pre-treatment, $^{16}O_2$ was used. Thus, CO_2 formed from $^{13}C^{16}O$ and a ^{16}O atom indicates the contribution of the MvK mechanism. During the consecutive pulsing, isotope-labelled $^{18}O_2$ was pulsed. Thus, CO_2 formed from $^{13}C^{16}O$ and an ^{18}O atom can be associated with a contribution of the LH mechanism.

By varying the time delay between the oxygen ($t = 0$ s) and CO pulses ($t = 0$, 0.5, 1, 2, 4 s), the importance of residence time and adsorption strength of the reactants can be assessed. The height-normalised oxygen responses observed over $CuMnO_X$ and Au/$CuMnO_X$ catalysts are shown in Figs. 1 and 2, respectively. For both catalysts, the O_2 responses exhibit the same shape when CO pulses were delayed by 0.5, 1, 2 and 4 s. In the case of simultaneous pulsing of O_2 and CO, the oxygen responses are narrower indicating depletion of oxygen due to more intensive reaction with CO that immediately adsorbs on the catalyst surface. Over both catalysts, oxygen adsorbed reversibly as is further detailed from the multi-pulse experiments described later. For both catalysts, the O_2 response decays rapidly over the first 0.5 s and, after 1 s, no more gaseous oxygen remains in the reactor. At this point, only irreversibly adsorbed oxygen participates in the reaction. The latter surface oxygen is usually associated with the MvK mechanism.

Figs. 3 and 4 report the argon-normalised CO responses observed when CO was pulsed with different time delays (0, 0.5, 1, 2 and 4 s) over the $CuMnO_X$ and Au/$CuMnO_X$ catalysts, respectively. Clearly, the responses are much broader, indicating strong reversible adsorption of CO, which required a relatively long observation interval of 30 s to cover the timeframe over which gaseous CO remained in the reactor.

Figs. 5 and 6 report argon-normalised $^{13}C^{16}O^{16}O$ and $^{13}C^{18}O^{16}O$ responses observed when $^{13}C^{16}O$ was pulsed with different time delays over $CuMnO_X$ and Au/$CuMnO_X$ catalysts, respectively. It was found that regardless of the time delay between $^{18}O_2$ and $^{13}C^{16}O$ pulses, the major CO_2 isotope produced in the reaction was $^{13}C^{16}O^{16}O$ (AMU 45) followed by $^{13}C^{18}O^{16}O$ (AMU 47). A small amount of $^{13}C^{18}O^{18}O$ (AMU 49) was also observed. This doubly labelled CO_2 could be formed during CO_2 re-adsorption and exchange with surface-labelled oxygen which was confirmed in a separate experiment.

The production of CO_2 with both unlabelled oxygen atoms is a clear fingerprint of the MvK mechanism because the source of unlabelled oxygen is the initial pre-oxidation. The production of CO_2 with one ^{18}O atom indicates that pulsed double-labelled oxygen $^{18}O_2$ also participates in the reaction. This would indicate that some vacancies/sites of/from active surface oxygen are refilled by dissociative adsorption from the gas phase. Such a reaction step is characteristic of the LH mechanism. It may also occur within the MvK mechanism if some very active oxygen sites are present in an amount that is comparable with the amount of oxygen pulsed. A typical consecutive pulsing experiment included about 200 pulses for reasonable averaging of observed responses. A typical O_2 pulse intensity was kept in the range of $1.5–2 \times 10^{-10}$ mol/mg of catalyst that makes a total amount of oxygen molecules pulsed of around $3–4 \times 10^{-8}$ mol/mg. In oxygen multi-pulse experiments, it was found that after 100 pulses or consumption of about 2×10^{-8} mol/mg of oxygen atoms, the O_2 adsorption constant drops significantly (by about a factor of 5). A similar amount of sites were found to be very active in CO oxidation during CO multi-pulse experiments. Thus, the amount of oxygen pulsed during consecutive pulsing is comparable with the amount of adsorption sites/active surface oxygen.

Fig. 7 reports the yield of different CO_2 isotopes observed over $CuMnO_X$ and Au/$CuMnO_X$ catalysts plotted as a function of time of the delay of the CO pulse. The comparison of the CO_2 yields clearly shows that the Au-doped catalyst is more active than the undoped $CuMnO_X$ catalyst. Remarkably, this increase in activity comes from the increased production of the CO_2 isotope with both unlabelled oxygen atoms implying that the gold doping promotes the MvK mechanism. However, the fact that the CO_2 yield depends on the time delay between the CO and the O_2 pulses indicates that there is a contribution from both LH and MvK reaction mechanisms. The yield of $^{13}C^{16}O^{16}O$ (AMU 45) does not depend on the time delay as expected for the MvK mechanism. The yield of $^{13}C^{18}O^{16}O$ (AMU 47) rapidly decreases within one second and then stays approximately constant. As was concluded from the analysis of oxygen responses, after one second no more gaseous oxygen remains in the TAP reactor. The CO pulse injected after 1 s can then only react with surface oxygen irreversibly adsorbed prior to the CO pulse. Such irreversibly adsorbed oxygen can be associated with either LH or MvK mechanisms, which can be hard to distinguish based on kinetic data from these experiments. Clearly, reaction with such oxygen should not depend on the time delay between the pulses, as long as it is $\geqslant 1$ s.

Higher production of $^{13}C^{18}O^{16}O$ in the case of simultaneous pulsing (compared with the cases of longer time delays) indicates that reversibly adsorbed oxygen also participates in CO oxidation. This is a clear fingerprint of the LH mechanism.

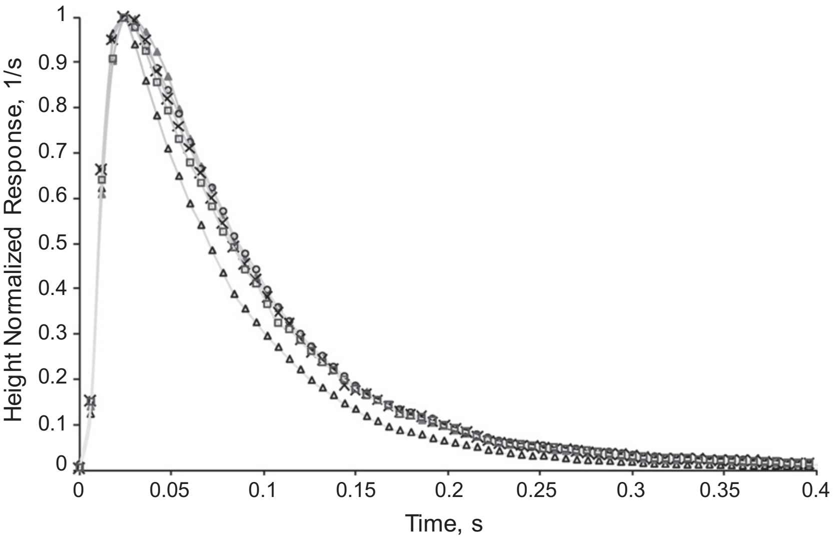

Fig. 1. O2 pulse responses over $CuMnO_X$ when CO is pulsed after varied time delays (t): (-Δ-) $t = 0$ s, (-▲-) $t = 0.5$ s, (-○-) $t = 1$ s, (-x-) $t = 2$ s, (-□-) $t = 4$ s.

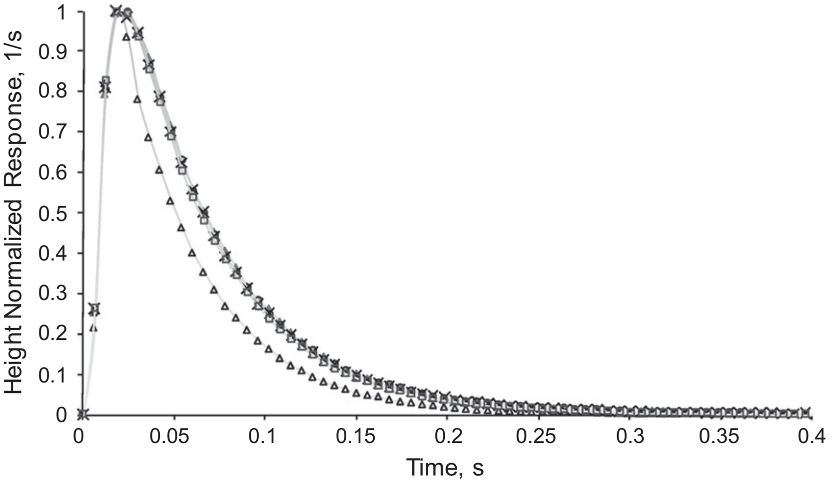

Fig. 2. O_2 pulse responses over Au/CuMnO$_X$ when CO is pulsed after varied time delays (t): (-Δ-) $t = 0$ s, (-▲-) $t = 0.5$ s, (-○-) $t = 1$ s, (-x-) $t = 2$ s, (-□-) $t = 4$ s.

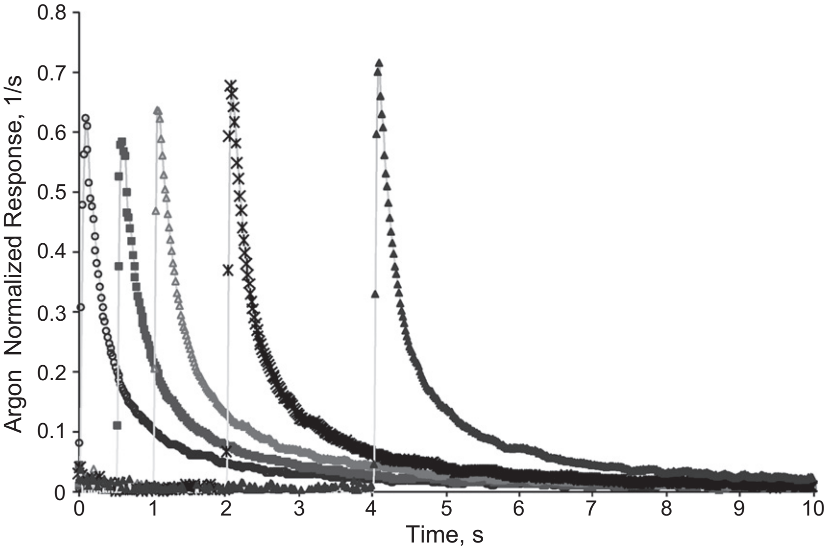

Fig. 3. CO responses over CuMnO$_X$ when pulsed after O_2 at varied time delay (t): (-○-) $t = 0$ s, (-■-) $t = 0.5$ s, (-Δ-) $t = 1$ s (-x-) $t = 2$ s, (-▲-) $t = 4$ s.

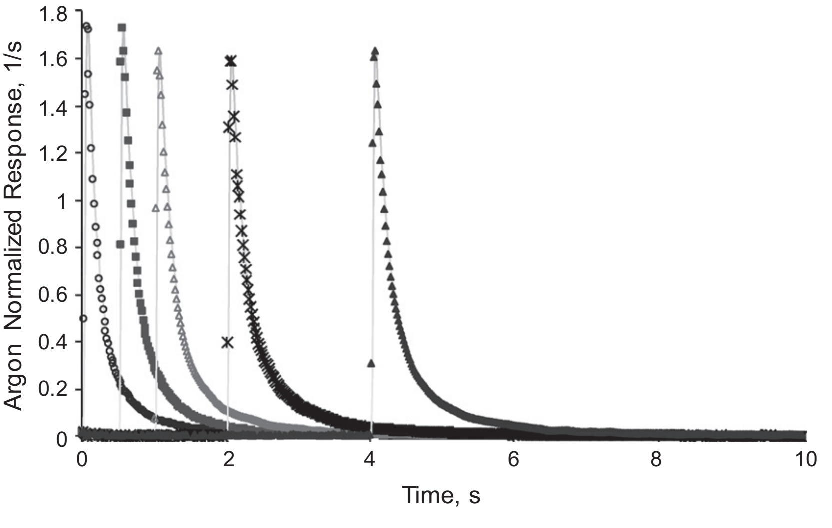

Fig. 4. CO responses over Au/CuMnO$_X$ when pulsed after O_2 at varied time delay (t): (-○-) $t = 0$ s, (-■-) $t = 0.5$ s, (-Δ-) $t = 1$ s (-x-) $t = 2$ s, (-▲-) $t = 4$ s.

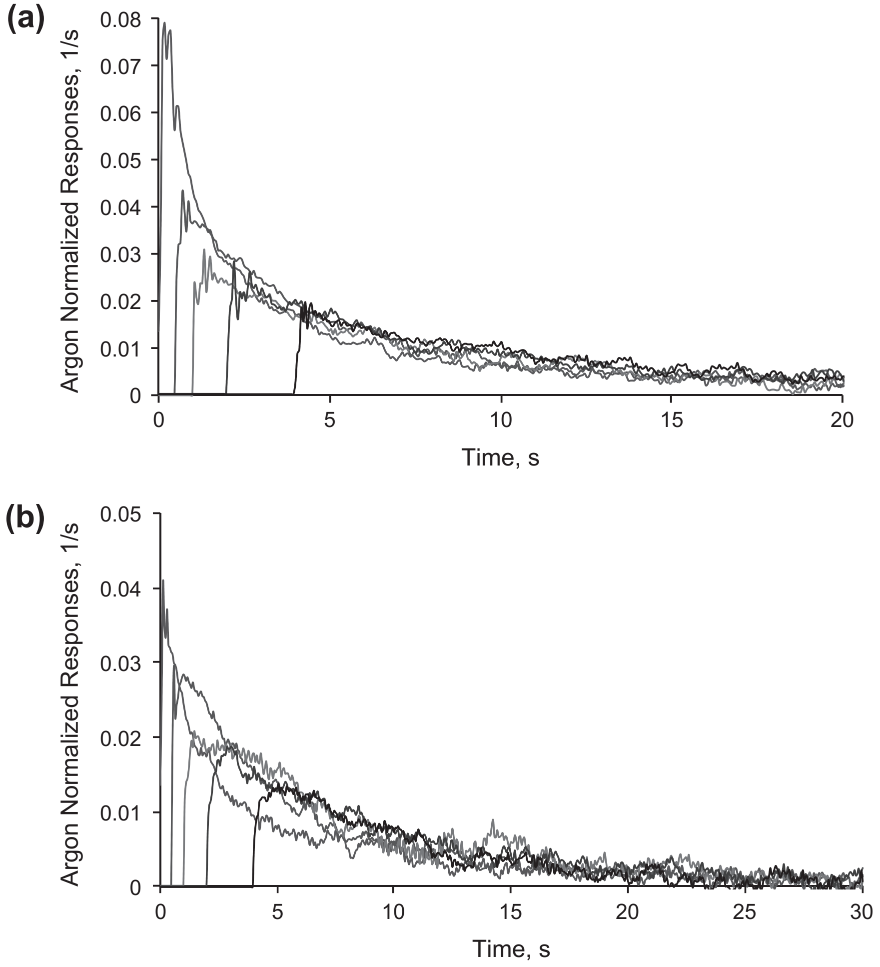

Fig. 5. CO_2 responses over $CuMnO_X$ as a function of the time interval between O_2 and CO pulses (a) AMU45 (b) AMU47; at $t = 0$, 0.5, 1, 2 and 4 s.

In summary, a larger contribution of the Mars van Krevelen mechanism and a smaller contribution of the Langmuir–Hinshelwood mechanism are observed for CO oxidation over both catalysts. The presence of gold doping does not significantly affect the LH mechanism contribution, whereas it clearly promotes the Mars van Krevelen mechanism compared with the undoped $CuMnO_X$ catalyst. This results in an increase in the overall CO oxidation activity of the 0.5% Au-doped $CuMnO_X$ catalyst.

5. Multi-pulse experiments

Utilisation of the thin-zone multi-pulse TAP experiment provides a method by which the catalyst composition may be changed in a controlled and gradual manner by exposing the catalyst to a large number of pulses of a reactant. The amount of reactant consumed and product formed can be monitored as a function of the pulse number or surface composition of the catalyst. In contrast, in a single-pulse kinetic test, the catalyst composition does not change significantly because the amount of pulsed molecules is much smaller than the number of surface active sites/species. Thus, in a multi-pulse experiment, it is possible to observe the whole dependence of the catalyst activity as a function of the catalyst composition or amount of available active sites. A detailed analysis of these dependencies enables the sites to be distinguished kinetically with respect to the progressive activity changes (i.e. decreases) as each site becomes occupied (see [10] for details of this concept).

From the consecutive pulsing experiments (Fig. 7), the major contribution to CO oxidation over the $CuMnO_X$ and $Au/CuMnO_X$ catalyst is due to the Mars van Krevelen mechanism. According to this mechanism, CO reacts with surface oxygen that can be placed on the surface in a separate step. Consequently, multi-pulse TAP experiments using CO or oxygen provide a very useful tool for measuring the number and activity of surface sites involved in such a mechanism.

After normal pressure oxidation, both catalysts were characterised by three multi-pulse TAP experiments that included a CO multi-pulse (#1) followed by an O_2 multi-pulse, followed by a second CO multi-pulse experiment (#2). Figs. 8 and 9 report the evolution of the single-pulse CO conversion and CO_2 yield as a function of the cumulative amount of CO consumed by the $CuMnO_X$ and $Au/CuMnO_X$ catalysts, respectively, during the first and second series of CO multi-pulse experiments. For both catalysts, the CO_2 yield closely follows the CO conversion indicating that in each single-pulse experiment the majority of CO molecules reacted form CO_2, i.e. the carbon balance is maintained. Thus, each CO molecule consumed removed one oxygen atom from the catalyst surface. For both catalysts, the total amount of CO consumed in the first multi-pulse series was greater than in the second series (which followed the oxygen multi-pulse).

A comparison of the two catalysts clearly shows that the activity and the total amount of CO consumed or CO_2 produced is much greater over the gold-doped catalyst: 1.02×10^{-8} mol/mg ($CuMnO_X$) vs. 2.19×10^{-7} mol/mg ($Au/CuMnO_X$) in the first CO multi-pulse series and 4.42×10^{-9} mol/mg ($CuMnO_X$) vs. 1.11×10^{-7}

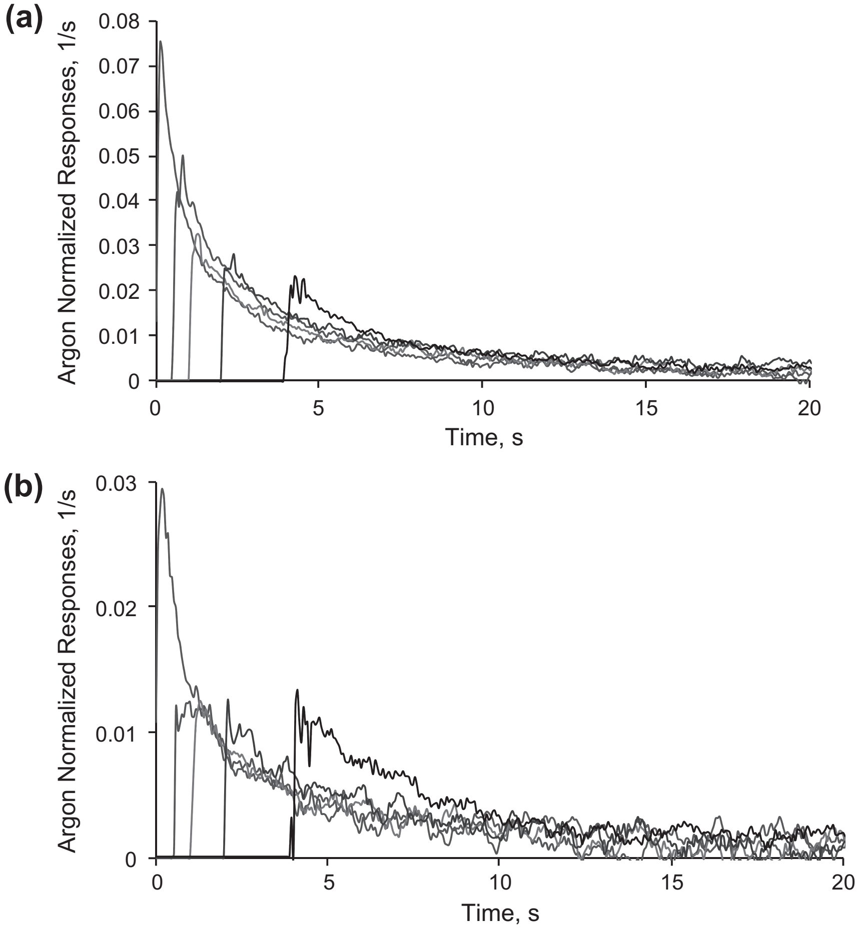

Fig. 6. CO_2 responses over Au/CuMnO$_X$ as a function of the time interval between O_2 and CO pulses (a) AMU45 (b) AMU47; at t = 0, 0.5, 1, 2 and 4 s.

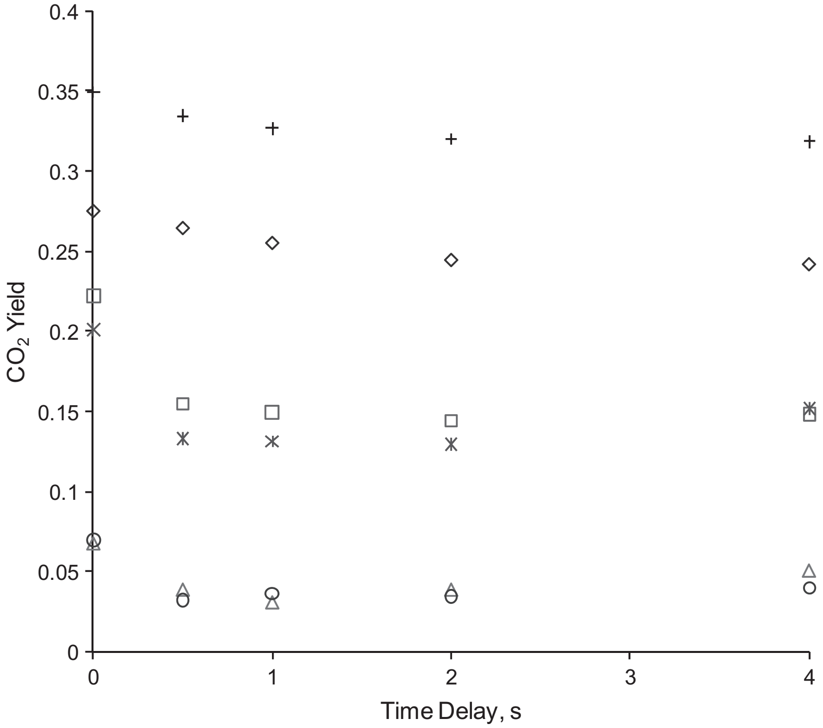

Fig. 7. CO_2 yields when CO is pulsed over CuMnO$_X$ and Au/CuMnO$_X$ catalysts at varied time delays after O_2 pulse: (◇) CO_2 (45) undoped, (+) CO_2 (45) Au doped, (□) CO_2 (47) undoped, (∗) CO_2 (47) Au doped, (Δ) CO_2 (49) undoped, (○) CO_2 (49) Au doped.

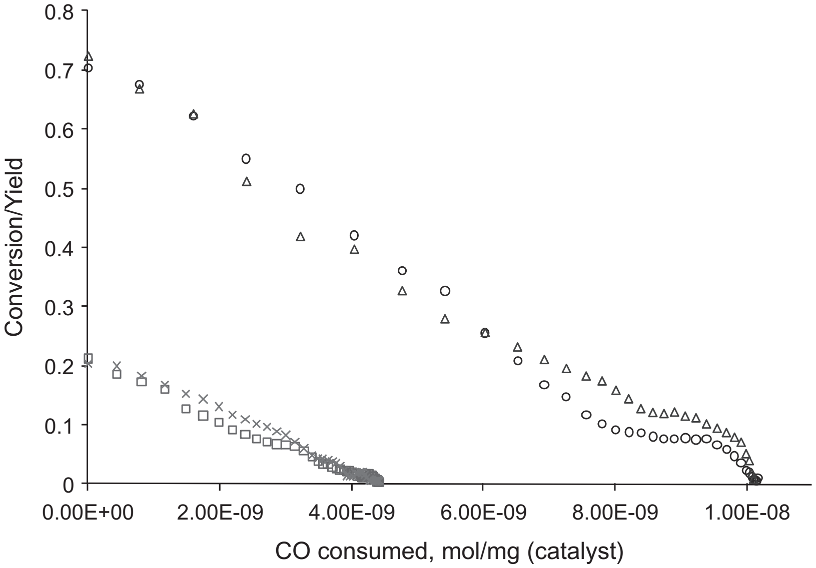

Fig. 8. Conversion (*X*) and yield (*Y*) observed in CO multi-pulse series over $CuMnO_X$ catalyst: (o) *X*, CO (1st series), (Δ) *Y*, CO_2 (1st series), (□) *X*, CO (2nd series), (x) *Y*, CO_2 (2nd series).

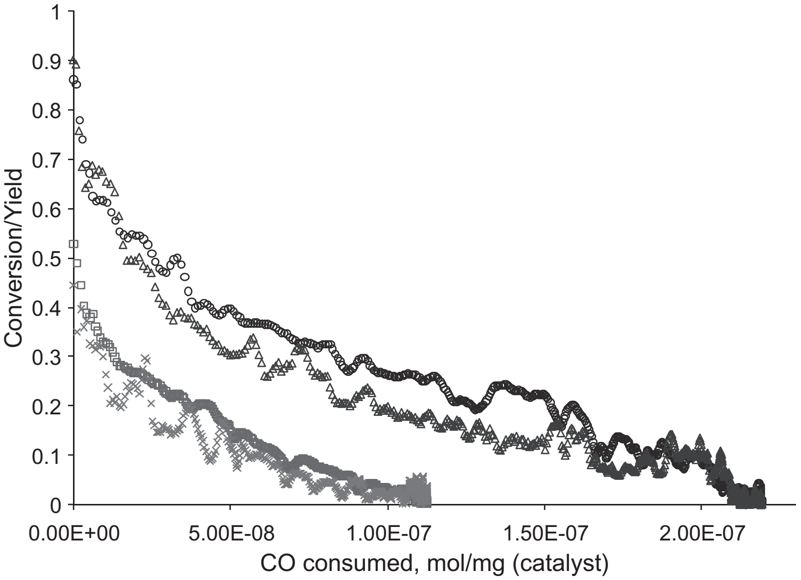

Fig. 9. Conversion (*X*) and yield (*Y*) observed in multi-pulse series over $Au/CuMnO_X$ catalyst: (o) *X*, CO (1st series), (Δ) *Y*, CO_2 (1st series), (□) *X*, CO (2nd series), (x) *Y*, CO_2 (2nd series).

mol/mg ($Au/CuMnO_X$) in the second CO multi-pulse series. Between these two CO multi-pulse series, both of the catalysts were re-oxidised by multi-pulsing oxygen. During the O_2 multi-pulse series, no CO_2 formation was observed, confirming the carbon balance mentioned earlier. Thus, only a small amount of inactive surface carbon/carbonate could have possibly been developed. Fig. 10 presents evolution of the single-pulse O_2 conversion as a function of the cumulative amount of oxygen atoms consumed by the $CuMnO_X$ and $Au/CuMnO_X$ catalysts. Again, the gold-doped catalyst exhibits higher activity in oxygen consumption and accumulates a slightly greater total amount of oxygen atoms: 9.68×10^{-8} mol/mg ($CuMnO_X$) vs. 1.08×10^{-7} mol/mg ($Au/CuMnO_X$).

It may be expected that the amount of CO consumed would be equal to the amount of oxygen atoms re-adsorbed during the subsequent O_2 multi-pulse. However, the amount of oxygen adsorbed in the multi-pulse series over the undoped catalyst was found to be about 10 times greater than the amount of CO consumed during either CO multi-pulse series. This means that most of the re-adsorbed oxygen remains in a form inactive for CO oxidation. The sites or vacancies for irreversible oxygen re-adsorption are likely to be dependent on the temperature at which the O_2 multi-pulse was performed i.e. 100 °C. The initial normal pressure oxidation was performed at 300 °C. At this temperature, it is likely that a fraction of sites exist that adsorb oxygen reversibly at that temperature, while at 100 °C these sites adsorb oxygen irreversibly. On the other hand, not all active oxygen was refilled by the oxygen multi-pulse series over the undoped catalyst, which is reflected by the lower activity and total amount of CO converted in the following second CO multi-pulse.

In contrast, in the case of the gold-doped catalyst, the amount of oxygen atoms adsorbed during the O_2 multi-pulse is smaller than the amount of CO consumed during the first CO multi-pulse series.

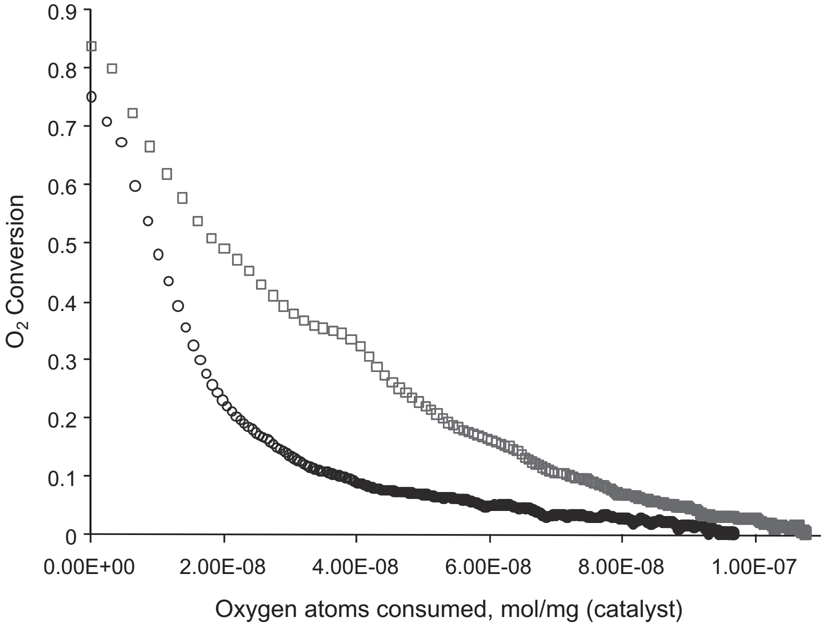

Fig. 10. Oxygen conversion over $CuMnO_X$ and $Au/CuMnO_X$ catalysts (o) O_2 $CuMnO_X$, (□) O_2 $Au/CuMnO_X$.

Remarkably, this amount is very similar to the amount of CO consumed during the second CO multi-pulse series. This means that not all active oxygen was refilled by the oxygen multi-pulse series over the gold-doped catalyst. However, all re-adsorbed oxygen was active for CO oxidation following re-oxidation of the catalyst.

In order to understand the difference between the two catalysts in terms of oxygen re-adsorption, a more detailed kinetic analysis of the oxygen responses was performed using moment-based formalism. The details including mathematical formulae can be found in [10]. The interaction of gaseous oxygen with the catalyst surface was described by the following sub-mechanism:

$$O_2 \underset{k_d}{\overset{k_a}{\rightleftarrows}} O_{2,ads}$$

$$O_{2,ads} \xrightarrow{k_{trans}} \text{Intermediate}$$

In this sub-mechanism, the first step is responsible for the reversible adsorption of oxygen, which was justified by comparing oxygen and argon responses. The second step is responsible for the transformation of reversibly adsorbed oxygen into irreversibly adsorbed species (intermediate) which does not leave the reactor in a gas form. Fig. 11 presents the rate constants calculated for each step of the O_2 sub-mechanism, plotted as a function of the cumulative amount of oxygen atoms consumed by the $CuMnO_X$ and $Au/CuMnO_X$ catalysts. It can be seen that the evolution of the oxygen adsorption constants is similar for both catalysts: it decreases from a maximum value at the beginning to zero at the end of the multi-pulse experiments, at which point the catalysts stops consuming oxygen. It takes about 2×10^{-8} mol/mg of oxygen atoms adsorbed for a significant drop of the adsorption constant. Afterwards, both catalysts accumulate oxygen in similar quantities (*ca.* 1×10^{-7} mol/mg). These adsorption sites cannot be associated with the gold which amounts to (assuming 100% dispersion) around 2.5×10^{-8} mol/mg of catalyst.

The desorption rate constants are also very similar and stay approximately constant during the whole multi-pulse series. The key difference is observed in terms of the transformation constant, k_{trns}. While slightly decreasing during the multi-pulse series, this constant is clearly higher in the case of $Au/CuMnO_X$ than for undoped $CuMnO_X$. This means that the Au doping promotes the transformation of reversibly adsorbed oxygen into irreversibly adsorbed surface species. Importantly, this irreversibly adsorbed oxygen is active for CO oxidation as follows from the results of the second CO multi-pulse experiment over the gold-doped catalyst.

The CO responses were also analysed using moment-based formalism [10]. Very broad CO responses were observed during consecutive and multi-pulse experiments, which suggested strong reversible adsorption of CO. This step combined with the surface reaction of adsorbed CO with the surface oxygen produces the following sub-mechanism for CO multi-pulse data analysis:

$$CO \underset{k_d}{\overset{k_a}{\rightleftarrows}} CO_{ads}$$

$$CO_{ads} + O_{ads} \xrightarrow{k_r} CO_{2ads}$$

In the second step of this process, the amount of surface oxygen atoms is assumed to be in large excess compared with the amount of adsorbed CO generated by the small intensity pulses. Then, the surface reaction constant, k_r, includes the amount of surface oxygen atoms as a factor. Whether this step produces adsorbed or gaseous CO_2 does not affect the mathematical analysis of the CO responses.

Fig. 12 presents the desorption rate constants, k_d, calculated for the proposed CO sub-mechanism and plotted as a function of the amount of CO consumed by the $CuMnO_X$ and $Au/CuMnO_X$ catalysts. For both catalysts, this constant is similar (around 5 s^{-1}) and remains approximately constant during both of the CO multi-pulse series (#1 and #2).

Fig. 13 shows the product of the adsorption constants (k_a) and the diffusional residence time in the catalyst zone (T_{cat}), plotted as a function of the cumulative amount of CO consumed by the $CuMnO_X$ and $Au/CuMnO_X$ catalysts, respectively. This constant exhibits similar behaviour for both catalysts. In the first CO multi-pulse series, the adsorption constant initially decreases until 5–8 $\times 10^{-9}$ moles of CO are consumed per mg of catalyst. Then, the adsorption constant reaches a similar value and becomes constant. In the second CO multi-pulse series, the adsorption constant does not change significantly having a similar value for both catalysts, which is about half of the value observed in the first CO multi-pulse series. This indicates that the multi-pulse re-oxidation did not regenerate all of the sites (5–8 $\times 10^{-9}$ mol/mg of catalyst) that

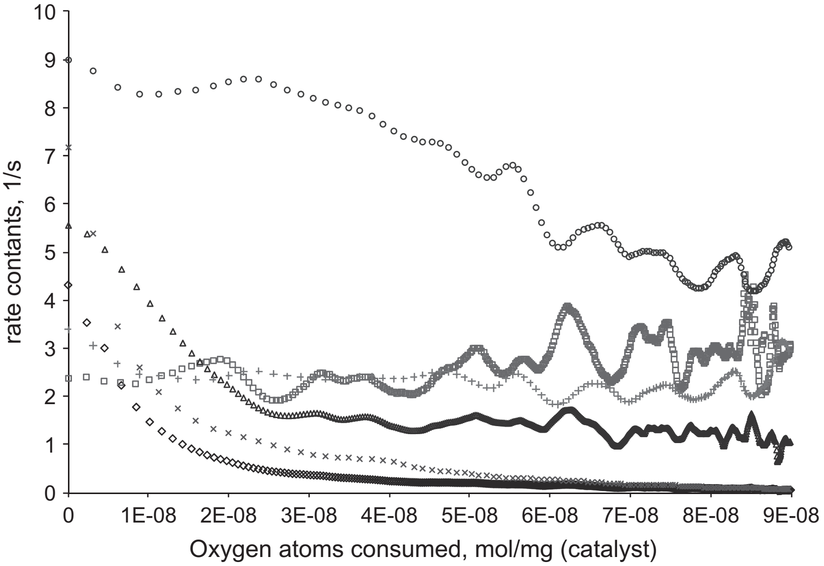

Fig. 11. Adsorption ($K_a * T_{cat}$), desorption (k_d) and transformation constants (k_{trns}) for CuMnO$_X$ and Au/CuMnO$_X$ catalysts: (◇) $K_a * T_{cat}$ O$_2$ CuMnO$_X$, (Δ) K_{trns} O$_2$ CuMnO$_X$, (□) K_d O$_2$ CuMnO$_X$, (x) $K_a * T_{cat}$ Au/CuMnO$_X$, (o) K_{trns} Au/CuMnO$_X$, (+) K_d O$_2$ Au/CuMnO$_X$.

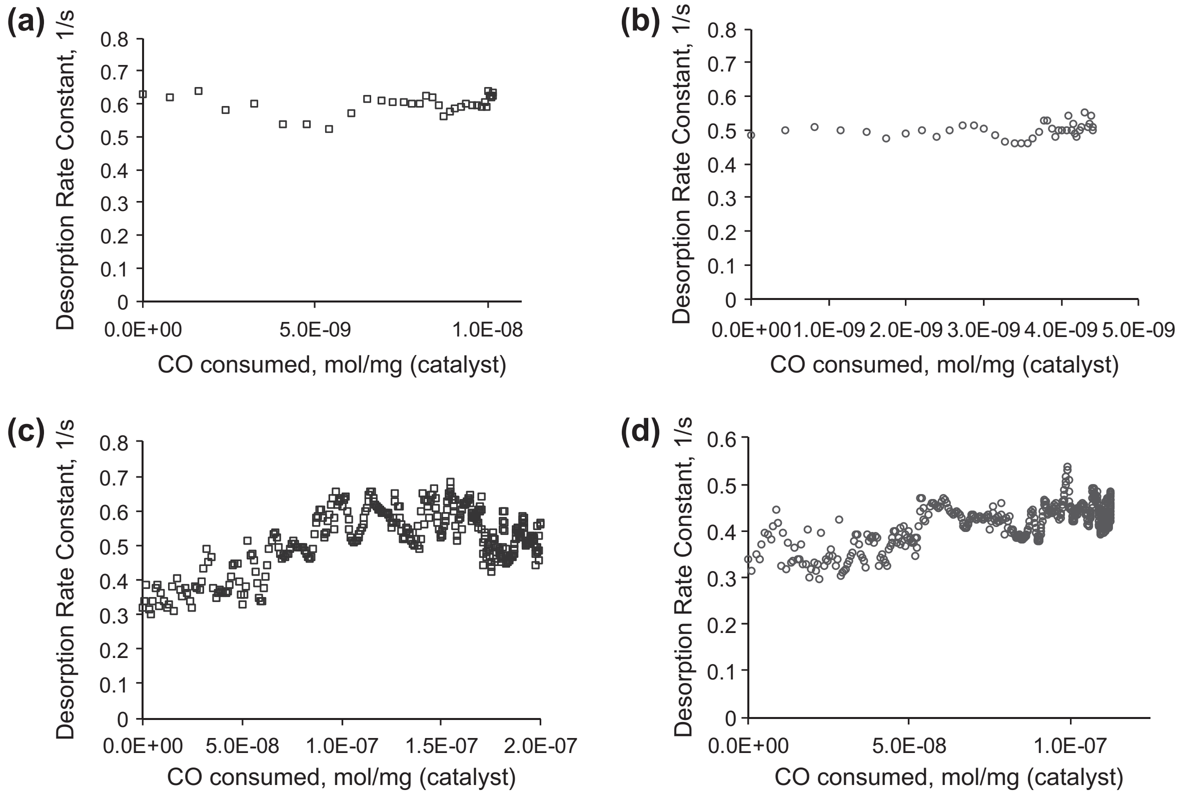

Fig. 12. CO desorption rate constants (k_d) vs. the amount of CO consumed by (a) CuMnO$_X$ 1st series (□), (b) CuMnO$_X$ 2nd series (o), (c) Au/CuMnO$_X$ 1st series (□), (d) Au/CuMnO$_X$ 2nd series (o).

were available at the beginning of the first CO multi-pulse series. In addition, the multi-pulse re-oxidation partly blocks the CO adsorption sites that were available at the end of the first CO multi-pulse series. This effect is observed for both catalysts.

Fig. 14 reports the surface reaction rate constants, k_r, plotted as a function of the cumulative amount of CO consumed by the CuMnO$_X$ and Au/CuMnO$_X$ catalysts.

For both catalysts and both CO multi-pulse series, this constant starts from a maximum value and decreases to zero at the end of each experiment. Both catalysts stop consuming/converting CO because the surface reaction no longer proceeds reflecting that no more active oxygen is available on the surface. This is consistent with the supposition that the multi-pulse re-oxidation only partly refills the surface of both catalysts with active oxygen.

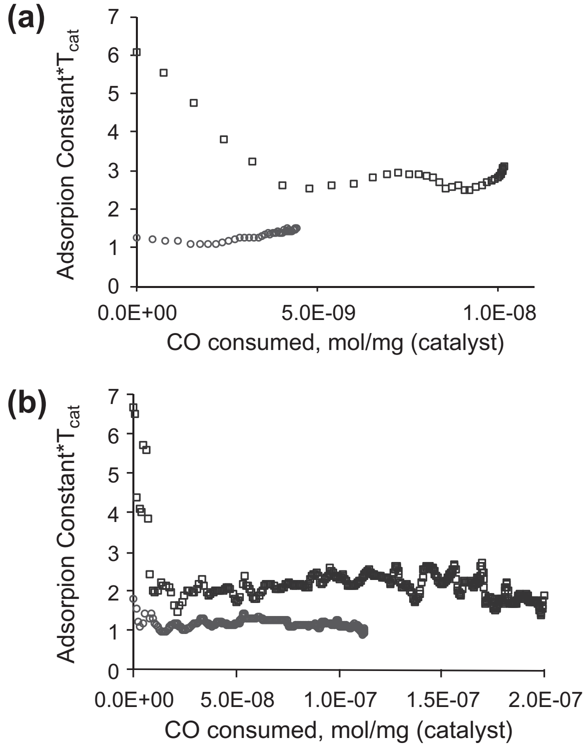

Fig. 13. CO adsorption constants (k_a) multiplied times residence time in the catalyst zone (T_{cat}) vs. the amount of CO consumed by the CuMnO$_X$ (a) and Au/CuMnO$_X$ (b) catalysts (□) 1st series, (o) 2nd series.

In terms of CO oxidation, the most interesting difference between the two catalysts is the surface reaction constant dependence on the amount of CO consumed/converted, which is equal to the amount of oxygen atoms removed from the catalyst surface as stated earlier. For the undoped catalyst, the surface reaction constant is approximately proportional to the amount of surface oxygen atoms available, i.e. the total amount of active oxygen atoms minus the amount of atoms removed. Such a dependence indicates that a single kind of active oxygen species participates in the CO oxidation i.e., all surface oxygen species involved have the same intrinsic activity.

In the case of the gold-doped catalyst, the dependence of the surface reaction constant is more complex. In this case, two distinct regions can be observed (marked by dashed lines). The first region (region 1) is located between 0 and 1×10^{-8} moles of CO consumed per mg of catalyst. In this region, a steep linear decrease in k_r is observed. The second region (region 2) follows the first one and continues until the end of the multi-pulse experiment. In region 2, k_r also decreases linearly but not as steeply as in region 1.

For a given catalyst, a linear decrease in k_r reflects that oxygen species of similar intrinsic activity dominate in the corresponding region of the multi-pulse series. The slope of each linear decrease reflects how quickly the rate constant decreases with each active oxygen being removed. It is directly related to the intrinsic activity of the oxygen species. The different slopes of the linear dependency indicate the presence of oxygen species with different activities: the greater the slope the more active the surface oxygen. Consequently, the two regions observed for the gold-doped catalyst can be associated with two distinct types of active oxygen: more active in the first region and less active in the second region.

It should be noted that overall activity is determined by the activity and the number of active sites. Hence, a direct comparison of the gradients of the slopes of both catalysts is only possible if the total number of active sites is normalised.

Comparison of the k_r dependence on the amount of CO converted (or oxygen atoms removed) clearly shows that region 1 is of a similar longitude (0.5–1 $\times 10^{-8}$ mol/mg of catalyst) in the case of both catalysts. The slopes are similar as well, indicating a similar kind of active oxygen reacting. For both catalysts, the surface oxygen corresponding to region 1 was partly refilled during the multi-pulse re-oxidation.

Region 2 is observed only for the doped catalyst. Therefore, the active oxygen corresponding to this region can be associated with the Au doping. This active oxygen is less active (lower slope) but greater in number (1–2 $\times 10^{-7}$ mol/mg of catalyst). The multi-

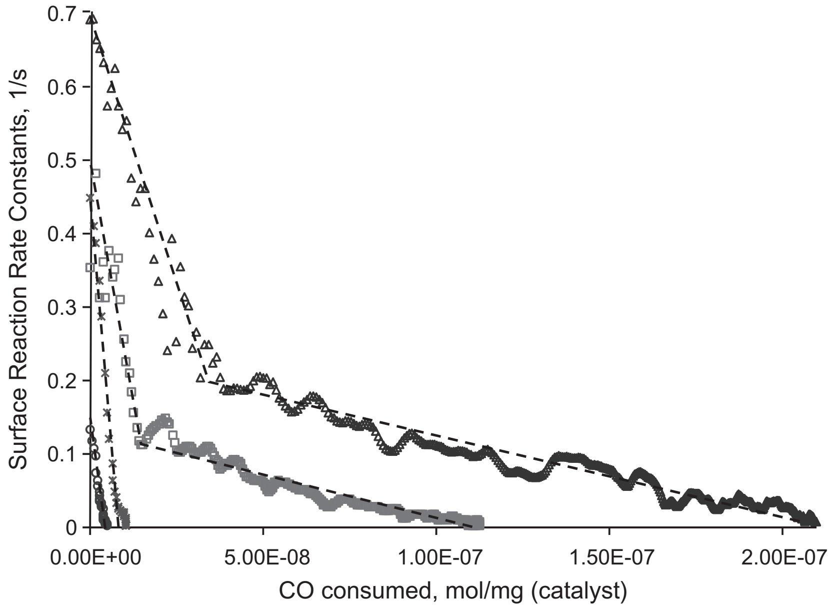

Fig. 14. CO surface reaction rate constants (k_r) vs. the amount of CO consumed by CuMnO$_X$ and Au/CuMnO$_X$ catalysts (•) k_r CuMnO$_X$ #1(o) k_r CuMnO$_X$ #2 (△) k_r Au/CuMnO$_X$ #1 (□) k_r Au/CuMnO$_X$ #2.

pulse re-oxidation refilled the surface oxygen corresponding to region 2 only partly.

6. Conclusions

Consecutive pulsing experiments have unraveled a higher contribution of the Mars van Krevelen mechanisms and a smaller contribution of the Langmuir–Hinshelwood mechanism in the CO oxidation reaction over undoped and gold-doped $CuMnO_X$ catalysts. The presence of gold doping does not affect significantly the contribution of the Langmuir–Hinshelwood mechanism. On the other hand, gold doping clearly promotes the Mars van Krevelen mechanism. This finding is in agreement with the results of the multi-pulse experiments. From the series of CO and O_2 multi-pulse TAP experiments, it has been deduced that gold doping modifies the catalyst surface so that it can store much more oxygen which is active for the CO oxidation. O_2 multi-pulse experiments have shown that gold doping primarily promotes the transformation of reversibly adsorbed or inactive surface oxygen into irreversibly adsorbed species that are active for CO oxidation via the Mars van Krevelen mechanism.

CO multi-pulse experiments have detected two distinct types of active oxygen species participating in the CO oxidation. This is in agreement with the findings of the consecutive pulse experiments which identified contributions of both Langmuir–Hinshelwood and Mars van Krevelen mechanisms. The first type of active oxygen was observed in a similar amount on both catalysts and was associated with the mixed oxide catalyst surface. The second type of active oxygen was found only on the gold-doped catalyst and was therefore clearly associated with the presence of gold on the catalyst surface. This type of active oxygen is less active in the reaction with adsorbed CO but is about 10 times greater in number than the amount of the active oxygen which is found on both catalysts. The catalyst is pre-treated in oxygen prior to the pulse experiments and then the amount of active oxygen is monitored by titrating the surface with oxygen following the CO multi-pulse. During this step, 10^{-7} moles of oxygen was taken up by the catalyst which is significantly greater than the available gold atoms even if the gold was 100% dispersed which equates to 2.54×10^{-8} moles in the sample. Therefore, the majority of the oxygen is used to oxidise the support. This oxygen is used in the conversion of CO; however, it is not clear whether the active oxygen is close to the gold centres or also involves atoms from the oxide far from the gold.

Acknowledgments

We would like to thank the EPSRC for funding as part of the Carmac and CASTech projects. Funding for studentships is acknowledged from DELNI (KM) and Molecular Products/EPSRC (KJC).

References

[1] B. Solsano, G.J. Hutchings, T. Garcia, S.H. Taylor, New J. Chem. 28 (2004) 708.
[2] D.R. Merrill, C.C. Scalione, J. Am. Chem. Soc. 43 (1921) 1982.
[3] T.H. Rogers, C.S. Piggot, W.H. Bahlke, J.M. Jennings, J. Am. Chem. Soc. 43 (1921) 1973.
[4] M. Haruta, N. Yamada, T. Kobayashi, S. Iijima, J. Catal. 115 (1989) 301.
[5] J.T. Gleaves, J.R. Ebner, C. Kuechler, Chem. Eng. Sci. 30 (1988) 49.
[6] G.J. Hutchings, A.A. Mirzaei, R.W. Joyner, M.R.H. Siddiqui, S.H. Taylor, Appl. Catal. A 166 (1998).
[7] A.A. Mirzaei, H.R. Shaterian, R.W. Joyner, M. Stockenhuber, S.H. Taylor, G.J. Hutchings, Catal. Commun. 4 (2003) 17.
[8] C. Jones, K.J. Cole, S.H. Taylor, M.J. Crudace, G.J. Hutchings, J. Mol. Catal. A 305 (2009) 121.
[9] A. Goguet, S.O. Shekhtman, R. Burch, C. Hardacre, F.C. Meunier, G.S. Yablonsky, J. Catal. 237 (2006) 102.
[10] S.O. Shekhtman, A. Goguet, R. Burch, C. Hardacre, N. Maguire, J. Catal. 253 (2008) 303.
[11] S.O. Shekhtman, G.S. Yablonsky, J.T. Gleaves, S. Chen, Chem. Eng. Sci. 54 (1999) 4371.
[12] S.O. Shekhtman, G.S. Yablonsky, Ind. Eng. Chem. Res. 44 (2005) 6518.
[13] S.O. Shekhtman, G.S. Yablonsky, J.T. Gleaves, R. Fushimi, Chem. Eng. Sci. 58 (2003) 4843.